

Electronic Supplementary Information

**Novel fabrication of nitrogen-doped mesoporous TiO<sub>2</sub> – nanorod titanate heterojunction to enhance photocatalytic degradation of dyes under visible light**

**Minh-Tri Nguyen-Le, Byeong-Kyu Lee\***

Department of Civil and Environmental Engineering, University of Ulsan, Nam-gu,

Daehak-ro 93, Ulsan 680-749, Republic of Korea

\* Tel: 82-52-259-2864, Fax: 82-52-259-2629, E-mail address: [bklee@ulsan.ac.kr](mailto:bklee@ulsan.ac.kr)

## **Experimental Section**

### **1. Chemicals.**

Ethylenediaminetetraacetic disodium salt (EDTA-Na<sub>2</sub>), acetic acid, titanium (IV) isopropoxide, isopropanol (ISP), tert-butanol (t-BuOH), p-benzoquinone (BQ), methylene blue (MB) were purchased from Sigma-Aldrich and were used for experiments without further purification. Deionized (DI) water from a Millipore water (18 MΩ.cm) purification system was used for all experiments.

### **2. Catalyst preparation.**

Briefly, 3.60 g of EDTA-Na<sub>2</sub> was dissolved in 100 mL of deionized water mixed with acetic acid (1.40 mL). A 50.0 mL mixture (1:2) of titanium (IV) isopropoxide precursor and isopropanol was then added dropwise to the prepared solution of EDTA-Na<sub>2</sub> under vigorous stirring at 4 °C for 3 h. The suspended solution was placed in the dark for 24 h. Afterwards, the suspension was transferred to a rotary evaporator to allow solvent evaporation in vacuum at 70 °C for 1 h, followed by drying in an oven at 105 °C. The dry sample was further calcinated at 400 °C for 3 h with a heating rate of 3 °C/min and ground into powders using a mortar. The sample thus obtained was denoted as C-TNR@N-TiO<sub>2-x</sub>. For comparison, the pristine TiO<sub>2</sub> was synthesized using the same process but in the absence of EDTA-Na<sub>2</sub>. All reagent-grade chemicals were used without pretreatment.

### **3. Characterization.**

The morphology of the as-synthesized materials was captured by using Field emission - scanning electron microscopy (FE-SEM) coupling with Energy – dispersive X-ray (EDX) spectroscopy. The specific Brunauer-Emmett-Teller (BET) surface area and pore size measurements of the samples were conducted on a Micromeritics ASAP 2020 apparatus under nitrogen atmosphere. The pore size distribution was calculated from Barrett-

Joyner-Halenda (BJH) desorption branches of isotherms. The crystal phases of the as-synthesized samples were analyzed by X-ray diffraction (XRD) patterns using a Bruker D8 advance powder diffractometer model (Copper anode, working condition: 40kV/ 30mA, scanning type: continuous scanning,  $2\theta = 10 - 70^\circ$ ). Raman spectra of samples were recorded on a LabRam HR micro-Raman instrument with a 532 nm Ar<sup>+</sup> ion laser at a room temperature. The chemical composition of the samples was analyzed based on X-ray photoelectron spectroscopy (XPS) data recorded on a Thermo Scientific Sigma Probe spectrometer with a monochromatic AlK $\alpha$  source (photon energy 1486.6 eV), spot size 400  $\mu\text{m}$ , pass energy of 200 eV and energy step size of 1.0 eV. For high resolution XPS spectra of elemental components, pass energy 50 eV and energy step size 0.10 eV were used. Triplicate scanings were performed with an accuracy  $\pm 0.2$  eV. For all samples, the C1s peak level was taken as an internal reference at 284.6 eV. All reported binding energy data were taken from high resolution XPS spectra. XPS peaks were deconvoluted by using symmetric Gaussian (Lorentzian) fitting curves. To verify the working optical range of samples, the UV-Vis diffuse reflectance spectroscopy (DRS) results of the samples were recorded on a Perkin-Elmer Lambda UV-Vis-NIR spectrophotometer. Photoluminescence (PL) spectra were collected at room temperature on a PTI luminescence spectrometer with a solid accessory. A Genesis 10S UV-Vis spectrophotometer was used to obtain the absorbance of the MB solution at 665 nm.

#### **4. Photocatalytic activity test.**

Methylene blue (MB) was used as a testing dye to evaluate the photocatalytic activity of the catalysts. Prior to irradiation with visible light, 20 mg of the synthesized catalyst was dispersed into 20 mL of 10 mg/L MB solution placed in a 100 mL quartz photo-reactor equipped with a circulating water system. The mixture was put in the dark condition under vigorous stirring for 30 mins to obtain adsorption-desorption equilibrium. The reactor was

then irradiated with a fluorescent lamp (Philips, 14 W, 1 mW/ cm<sup>2</sup>, ~ 10 cm above the MB solution) for 2 h. During irradiation, aliquots of MB were taken out at specific time intervals, and centrifuged at 3,000 rpm for 5 mins to remove any solids. The remaining MB concentration was determined using a UV-Vis spectrophotometer. All experiments were conducted at a room temperature. For quality assurance and quality control of measurements, a blank sample (only MB, without catalysts) was performed in the same conditions.

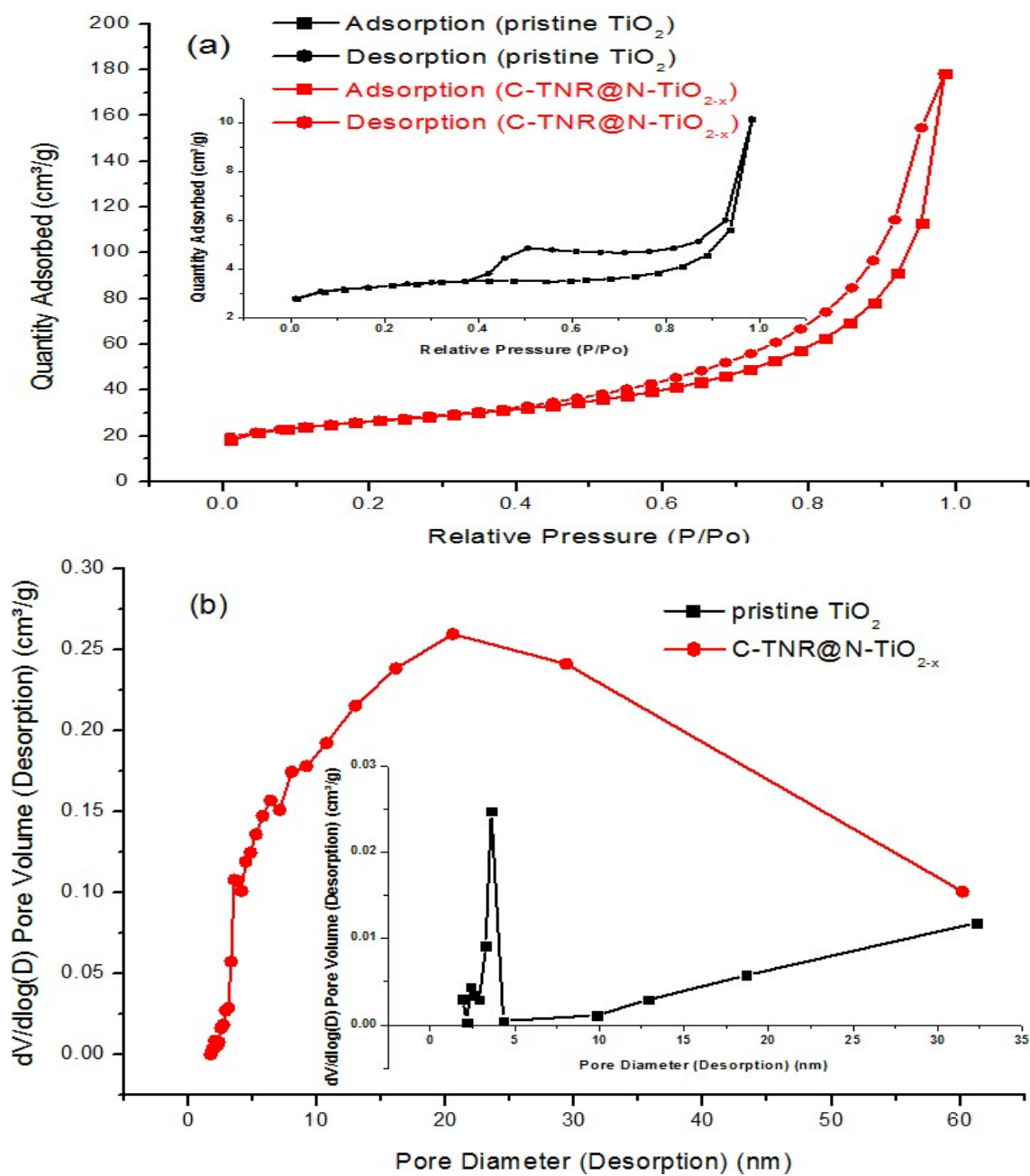


**Fig. S1** (a) Nitrogen adsorption-desorption isotherms and (b) pore size distribution of the C-TNR@N- $\text{TiO}_{2-x}$  and pristine  $\text{TiO}_2$ .

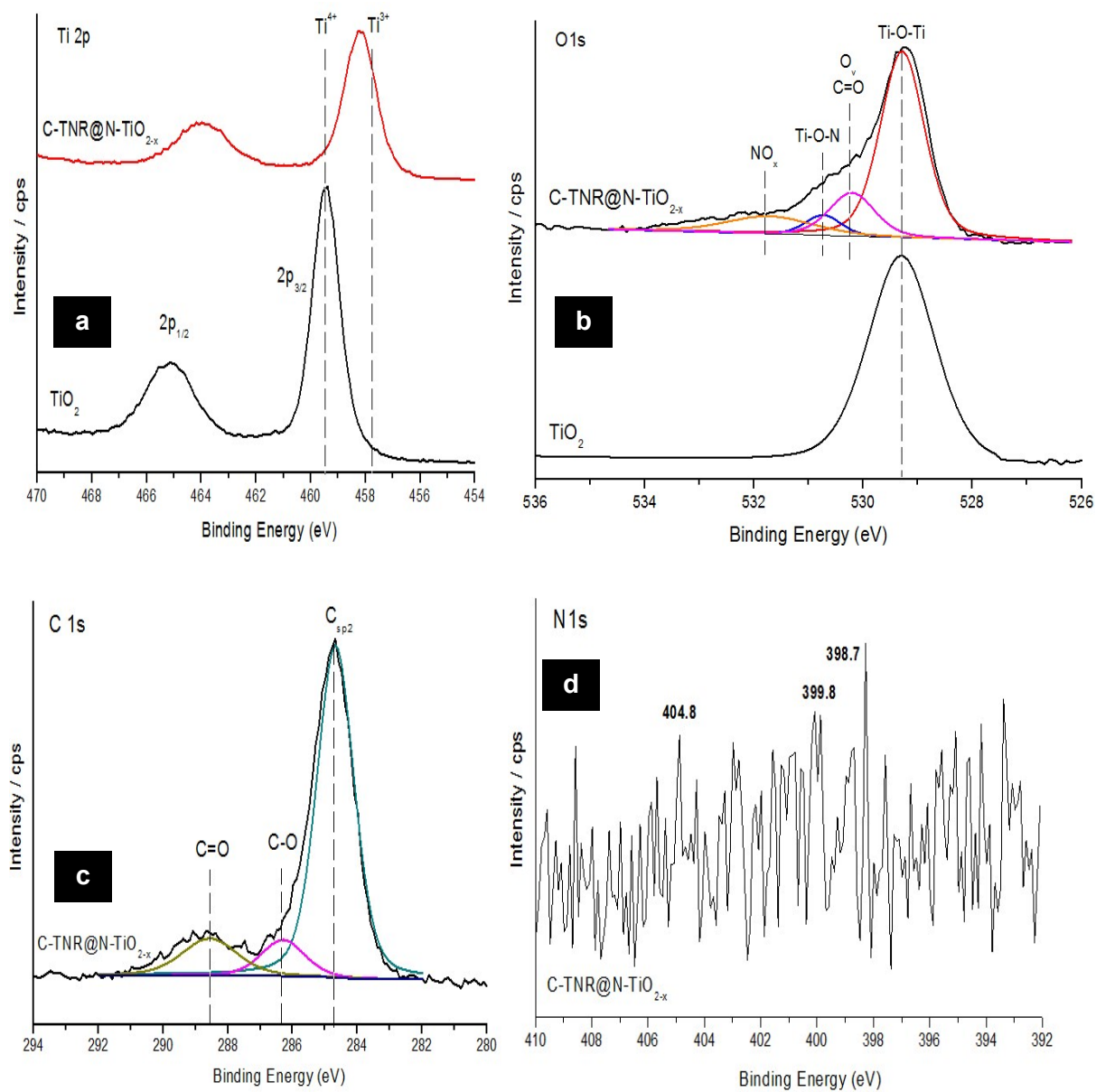


**Fig. S2** XPS spectra details for **(a)** Ti 2p level, **(b)** O 1s level, **(c)** C 1s level and **(d)** N 1s level of C-TNR@N-TiO<sub>2-x</sub> and pristine TiO<sub>2</sub>.

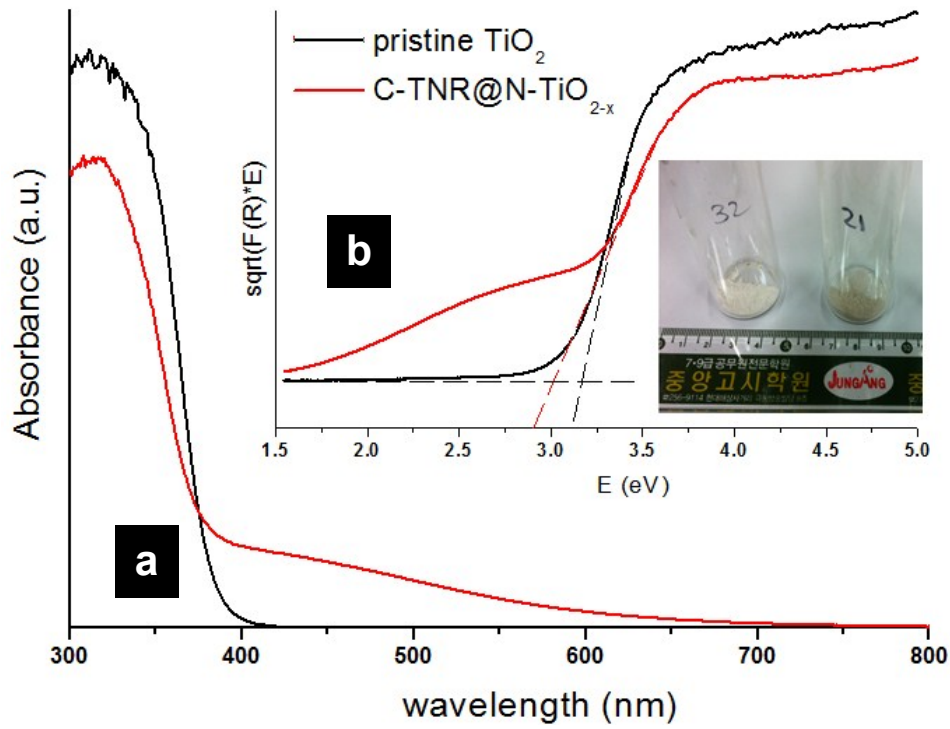


**Fig. S3 (a)** UV-Vis spectra for  $\text{C-TNR@N-TiO}_{2-x}$  and pristine  $\text{TiO}_2$ . **(b)** Band gap energy of both samples (obtained from the Kubelka – Munk plot). The inset: images for the pristine  $\text{TiO}_2$  and  $\text{C-TNR@N-TiO}_{2-x}$ .

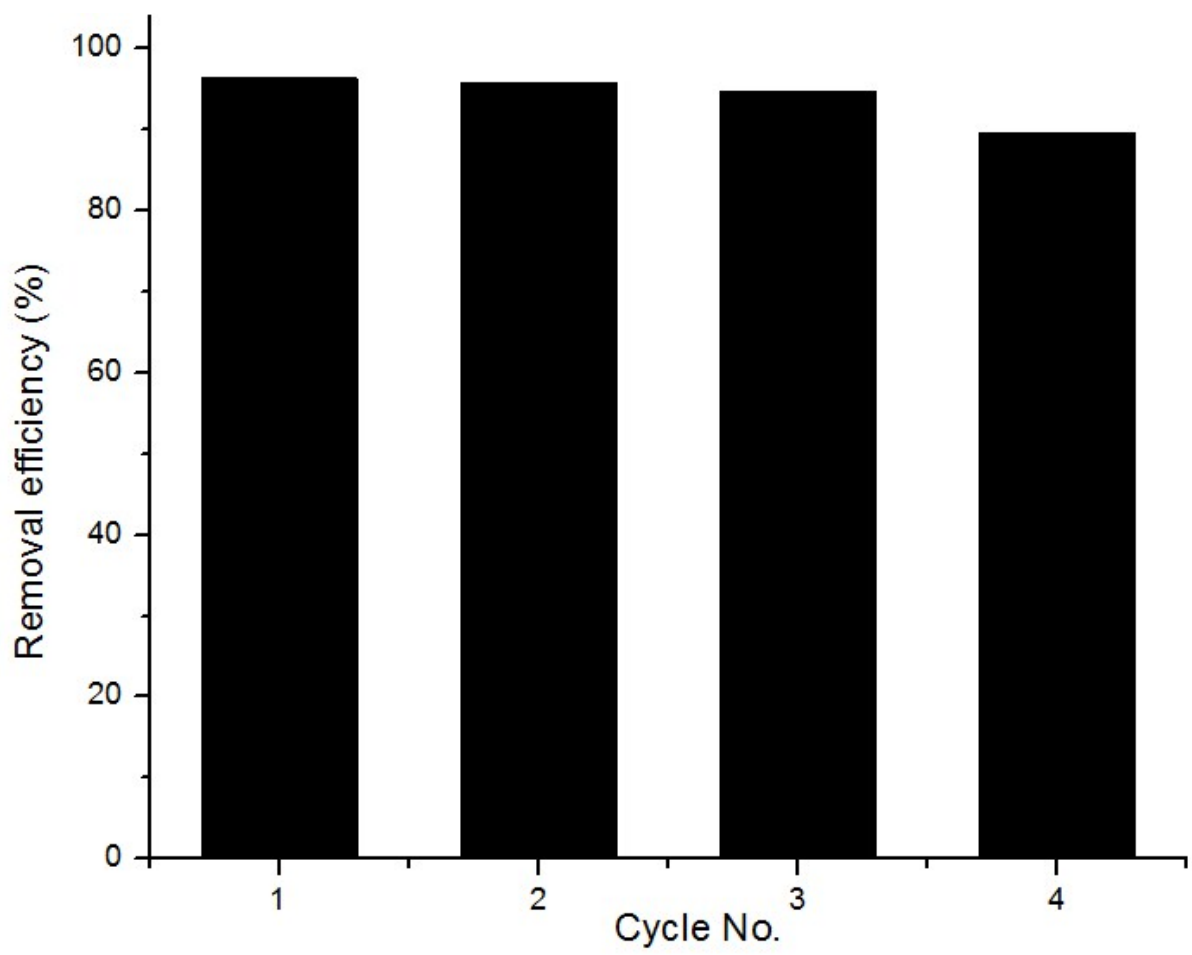


**Fig. S4** Photocatalytic removal efficiency of MB by C-TNR@N-TiO<sub>2-x</sub> at each cycles of reuse.



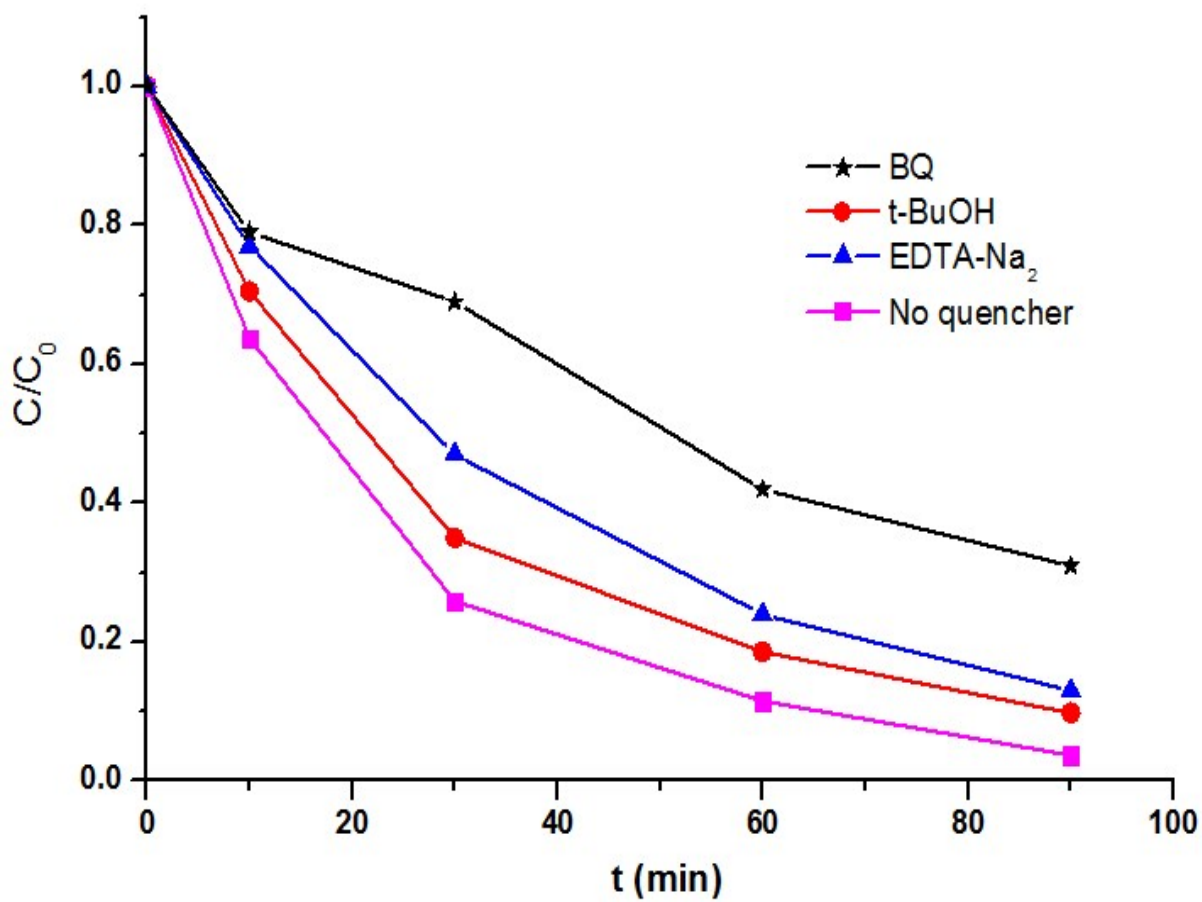


**Fig. S5** Photocatalytic degradation of 20 mL of 10 mg/L MB on C-TNR@N-TiO<sub>2-x</sub> in the presence of different scavengers.